

Claudia Barile, Caterina Casavola, Giovanni Pappalettera, Carmine Pappalettere

**RESIDUAL STRESS MEASUREMENT BY ELECTRONIC SPECKLE PATTERN  
INTERFEROMETRY: A STUDY OF THE INFLUENCE OF GEOMETRICAL PARAMETERS**  
**MERENJE ZAOSTALIH NAPONA ELEKTRONSKOM INTERFEROMETRIJOM ŠABLONA  
MRLJA: STUDIJA UTICAJA GEOMETRIJSKIH PARAMETARA**

Originalni naučni rad / Original scientific paper  
UDK /UDC: 539.4.014 620.179  
Rad primljen / Paper received: 9.10.2011

Adresa autora / Author's address:  
Politecnico di Bari, Dipartimento di Ingegneria Meccanica  
e Gestionale, Bari, Italy, [casavola@poliba.it](mailto:casavola@poliba.it)

**Keywords**

- residual stress
- ESPI
- integral method

*Abstract*

Hole drilling (HDM) is the most widespread method for measuring residual stress profile. HDM is based on the principle that a hole in the material causes a stress relaxation; stress field around the hole changes so that the released strain can be measured in order to calculate initial residual stress. Recently the use of optical methods as measurements tool of the strain field generated around the drilled hole has been investigated in place of the traditional strain gauge rosette technique. Optical methods have the advantage to guarantee very high sensitivity, to provide a much more significant statistic, to eliminate error due to hole eccentricity and to reduce the cost of the single test. The accuracy of the final result depends, among other factors, on the exact knowledge of the geometrical parameters of the measuring system. The exact knowledge of the illumination and detection angles influences, in fact, the accuracy in the determination of pixel size and sensitivity vector. The effect of an error in the measurement of geometrical parameters on final residual stress results is presented in this paper aside to some considerations about the accuracy in the zero position detection.

**INTRODUCTION**

Residual stresses are present in a material even in absence of an external load. They are introduced, in a mechanical part, as a consequence of manufacturing processes and they can affect fatigue behaviour, fracture strength and corrosion resistance, /1/. One of the most widespread method to measure residual stress is the hole drilling method using strain gauge rosettes /2, 3/. In this method stress relaxation is obtained by incrementally drilling a hole in the specimen. The resulting strain field is measured on the surface of the specimen by means of strain gauge rosette and finally residual stress, at each depth along the hole, is calculated. The method is ruled by an ASTM test standard, /4/. Stresses are related to measured strain by:

**Ključne reči**

- zaostali napon
- ESPI
- integralna metoda

*Izvod*

Bušenje rupa (HDM) je najraširenija metoda za merenje profila zaostalih napona. HDM se zasniva na principu da rupa u materijalu izaziva relaksaciju napona; naponsko polje oko rupe se menja tako da se oslobođena deformacija može izmeriti radi izračunavanja inicijalnog zaostalog napona. Upotreba optičkih metoda kao alata za merenje deformacionog polja koji se generiše oko izbušene rupe je nedavno proučena, umesto tradicionalne metode sa mernom deformacionom trakom, rozetom. Optičke metode imaju prednost koju garantuje vrlo visoka osetljivost, radi pružanja značajnije statistike, kojom se eliminiše greška usled ekscentričnosti rupe i smanjuje cena pojedinačnog ispitivanja. Tačnost konačnog rezultata zavisi, između ostalih faktora, od poznavanja tačnih geometrijskih parametara mernog sistema. Poznavanje tačnih uglova osvetljenja i detekcije, zapravo, utiče na tačnost u određivanju dimenzije piksela i vektora osetljivosti. Uticaj greške pri merenju geometrijskih parametara na konačne rezultate zaostalih napona je predstavljeno u ovom radu, pored nekih razmatranja tačnosti kod detekcije u nultom položaju.

$$\overline{\mathbf{G}}\overline{\boldsymbol{\sigma}} = \overline{\boldsymbol{\varepsilon}} \quad (1)$$

Where:  $\overline{\boldsymbol{\varepsilon}}$  is the vector of the strain measured by ESPI;  $\overline{\boldsymbol{\sigma}}$  is the vector of the corresponding stresses;  $\overline{\mathbf{G}}$  is a matrix whose  $G_{ij}$  elements represent the total surface deformation measured after  $i$ -depth increment caused by an unit stress within the  $j$ -depth increment.

The problem expressed by Eq.(1) can be solved by the least squared method:

$$\overline{\mathbf{G}}^T \overline{\mathbf{G}} \overline{\boldsymbol{\sigma}} = \overline{\mathbf{G}}^T \overline{\boldsymbol{\varepsilon}} \quad (2)$$

In principle any other technique able to measure strains could be coupled with the hole drilling method. In this context it seems to be appealing the use of optical methods. These methods allow, in fact, obtaining full field informa-

tion about strain at high resolution and high sensitivity. Many different methods have been used, until now, in combination with hole drilling: brittle and photoelastic coatings, moiré interferometry, holographic interferometry, electronic speckle pattern interferometry, interferometric strain rosette, digital image correlation and shearography, /5/. ESPI set up gives high precision and full field strain map and for these reasons it is supposed to be more accurate than strain gauge rosette. However, as every experimental technique, HDM + ESPI residual stress results could be affected by limitations inherent with the technique itself. The influence of these limitations, in particular the errors connected to uncertainty in determination of geometrical parameters and zero position detection are discussed in the following paragraphs.

## MATERIAL AND METHODS

### Experimental set-up for HDM + ESPI measurements

The ESPI hole-drilling measurement system (PRISM by Stresstech) used in this work is schematically reported in Fig. 1. A beam from a DPSS laser source is split into two beams and focused into two monomode optical fibres. One beam is collimated and illuminates the sample, while the second beam passes through a phase shifting piezoelectric system and then goes to the CCD camera where it interferes with the light diffused by the optically rough surface of the specimen. Initial phase and final phase are evaluated by the 4-step phase shifting technique, which allows to detect deformations released at each step of the hole-drilling process. The hole is drilled by means of a high speed turbine rotating at 35000 rpm which is mounted on a precision travel stage. The cutter is made by tungsten coated with TiN and has a nominal diameter  $d = 1.59$  mm. Experimental measurements are performed on a titanium grade 5 specimen (200 mm × 20 mm × 3 mm). Preliminary X-ray residual stress measurement is performed in order to evaluate the initial stress field on the specimen and it is found a very low value of about 10 MPa. Subsequently, the HDM + ESPI method is utilized to confirm this “unloaded” stress field (the hole is drilled till 0.8 mm depth in the centre of the specimen; each step was 0.16 mm).

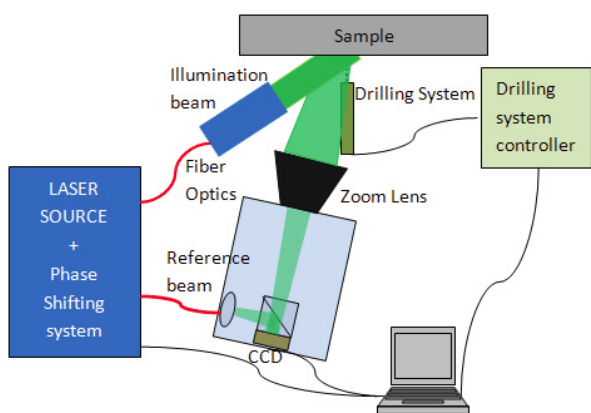


Figure 1. Experimental set-up for ESPI measurements of strains relaxed by HDM.

Slika 1. Shema eksperimentalnog ESPI merenja deformacija relaksiranih sa HDM

### Discussion on Zero Position

The first step in the residual stresses measuring procedure by means of HDM is to individuate the zero position, that is the very first contact of the cutter with the specimen surface before drilling starts. Correctly defining the zero position is a critical point in the entire measurement procedure because it represents the initial step of the drilling procedure. Residual stresses will be calculated at each step from strain released starting from this zero point, both using strain gauges and ESPI. In the case of the hole drilling strain gauge method, the zero point can be clearly defined by starting a very slow drilling procedure (0.01 mm/min) and stopping it immediately as the contact between cutter and specimen surface is reached. The contact information can be obtained through an electrical circuit or simply observing the surface of the rosette support wearing or, as last chance, monitoring in real time the change of strain values /4/. Anyway, it should be observed that a delay occurs between the contact information and the command to stop the drilling. This delay, inherent to the experimental technique itself, is hardly avoidable and could imply an error in residual stress evaluation. For this reason, in the case of hole drilling with ESPI method, three different methods are compared to determine the most accurate approach for determining the contact point between the cutter and the surface of the specimen. Three different procedures to define zero position are: (i) the method suggested by the manufacturer of PRISM<sup>®</sup>; (ii) the *AutoFind* method and (iii) the *Multimeter* method. The method suggested by manufacturer guidelines is a manual method strongly depending on the experience of the operator. The cutter moves toward the specimen at very low speed (0.05 mm/s); as soon as the cutter reaches the surface, a strong noise is produced. So the operator has to stop the movement of the translation stage that guides the driller and can define the zero position. The main drawback of this method is that it is strongly related to the promptness of the operator. Moreover, the noise produced during drilling operation depends on material type and on rotational speed, so it seems that noise is not a reliable parameter for detecting the contact point. The *AutoFind* method is an automatic method implemented in the software package of PRISM. The cutter moves forward the specimen while rotating at the lowest speed; when it touches the surface, the electric circuit cutter specimen-clamping system-earth is closed, the contact is reached, the translation and the rotation are stopped and the actual position is defined as zero-position. The main drawbacks of this method are that it can be used only for conductive materials and sometimes the contact is not properly detected, so the driller continues drilling the hole. The use of a *multimeter* represents a semiautomatic method. The driller moves toward the specimen but it does not rotate (and does not drill the hole). The probes of a multimeter are placed respectively on the driller and on the specimen. When the cutter reaches the surface, the multimeter indicates the contact and the operator stops the procedure and defines the zero point. The main drawback of this method is that it can be used only for conductive materials. Before starting experiments, the geometry of the specimen is evaluated. If the thickness of the

specimen is not uniform, the contact between cutter and surface occurs in different locations at different  $z$  position. This  $z$ -shifting could cause an error  $\Delta = (Z'' - Z')$  on the evaluation of the zero-position as shown in Fig. 2.

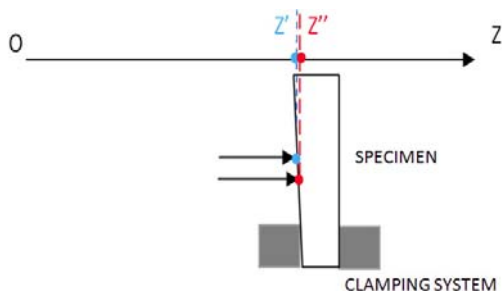


Figure 2. Schematic of the error on the zero position caused by specimen thickness variation.

Slika 2. Shema greške u nultom položaju izazvana promenom debljine uzorka

A Vernier calliper and a digital comparator are used in order to evaluate variation in thickness and surface irregularity. So, the calliper is used to evaluate thickness of the specimen. Finally, the specimen is positioned on a horizontal plane and clamped; a digital comparator is used to scan the surface along different lines in order to measure the magnitude of geometrical surface irregularities.

#### Discussion on HDM + ESPI geometrical parameters

The geometry and mutual position of laser, CCD and specimen should be accurately defined to correctly measure the strain map. The  $xyz$  reference system of the specimen and the  $x'y'z'$  reference system of the CCD camera are considered as shown in Fig. 3. To exactly calculate strains from measured displacements, it is necessary to evaluate the pixel size along  $x$  and  $y$  directions, this means that the angles of CCD camera with respect to the specimen reference system  $xyz$  are needed. The  $\alpha_2$  angle defines the  $x$  axis and the  $x'$  axis; the  $\beta_2$  angle defines the  $z$  axis and the  $z'$  axis; the  $\gamma_2$  angle defines the  $y$  axis and the  $y'$  axis.

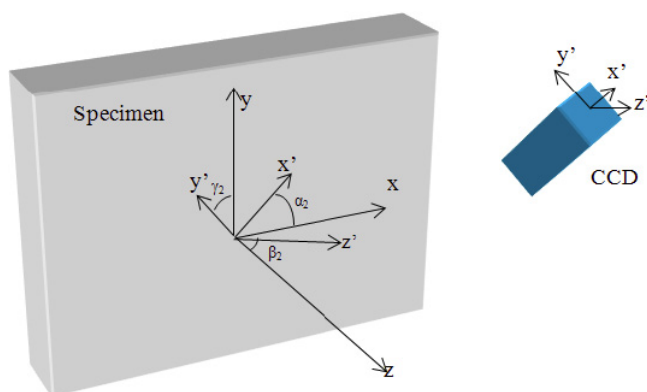


Figure 3. Schematic of the geometrical set-up with the CCD camera and specimen.

Slika 3. Shema geometrije sa CCD kamerom i uzorkom

Moreover, to calculate strains from measured displacements, it is necessary to know the phase changing of the pattern, detected during tests, and the sensitivity of the optical set up that depends on the geometry of the illumination system. Due to the cylindrical symmetry of the illumination

beam around the propagation direction of the laser, only two angles are necessary in this case to relate the specimen reference system and the illumination reference system. Being  $x''y''z''$  the illumination beam reference system, the  $\alpha_1$  angle defines the  $x$  axis and the  $x''$  axis, while the  $\beta_1$  angle defines the  $z$  axis and the  $z''$  axis. These geometrical angles can be initially measured by a goniometer. The uncertainty in this measurement is estimated to be  $\Delta = \pm 2^\circ$  because of the difficulties to correctly position the goniometer inside the measurement system. In order to assess the influence of an error in the measurement of the geometrical parameters on the results in terms of measured stress, a simple test is run. A 200 mm  $\times$  20 mm  $\times$  3 mm titanium specimen is subjected to three point bending and induced stresses are measured as shown in Fig. 4.

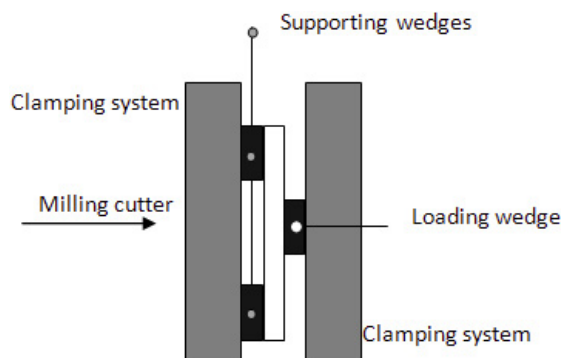


Figure 4. Top view of the three-point bending load frame.  
Slika 4. Pogled odozgo na sklop savijanja u tri tačke

The profile of the induced stresses is measured up to 0.8 mm depth. The angle values are  $\alpha_1 = 42.5^\circ$ ;  $\beta_1 = 0^\circ$ ;  $\alpha_2 = 24^\circ$ ;  $\beta_2 = 0^\circ$ ;  $\gamma_2 = 0^\circ$ . Then the stress profile is recalculated by hypothesizing an error  $\pm 2^\circ$  on each of the considered angles. Results of this analysis are presented in the next section.

## RESULTS

### Zero detection

Geometrical regularity of the specimen is detected on an area of 10 mm  $\times$  10 mm. The thickness of the sample is measured in several locations giving the following results:

Table 1. Thickness measured on a 10 mm  $\times$  10 mm specimen area  
Tabela 1. Debljina izmerena na površini uzorka 10 mm  $\times$  10 mm

Thickness (mm)	4.91	4.93	4.91	4.88	4.87	4.89	4.89	4.89

The average thickness of the sample is  $d_{ave} = 4.90$  mm with a standard deviation  $\sigma_d = 17.8 \mu\text{m}$ .

Macroscopic surface irregularities are evaluated by means of a digital comparator. Table 2 reports the height ( $z$ ) measured at different positions along a diagonal of the specimen.

The standard deviation of this set of measurements provides an estimation of surface irregularities:  $\sigma_z = 8.86 \mu\text{m}$ .

Table 2. Height measured at points along a diagonal of the sample.  
Tabela 2. Izmerena visina duž tačaka dijagonale uzorka

$z$ ( $\mu\text{m}$ )	-7.44	4.28	8.03	3.65	12.83	-6.85	-15.59	-6.95	0.90	7.18

Geometrical considerations on specimen surface irregularities and on cutter allow evaluating the precision of the method of zero detection suggested by manufacturer. If we consider the geometry of the cutter shown in Fig. 5 and we take into account that the radius of the cutter is  $r = 0.8$  mm while the angle of the cutting edges is  $3^\circ$ , it is possible to calculate the height of the cutting edges  $h = 41.9$   $\mu\text{m}$ . Using the method of zero detection suggested by the manufacturer, the operator should stop the cutter movement before the depth of  $h = 41.9$   $\mu\text{m}$  is reached. This is easily verified by checking the trace on the specimen: it should appear as an annulus.

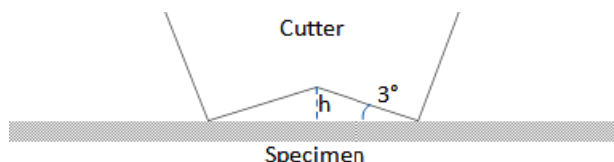


Figure 5. Schematic of the cutter geometry.  
Slika 5. Shema geometrije sekača

Unluckily, this observation cannot be done in real time, so the error that can be accomplished with this method is just  $h = 41.9$   $\mu\text{m}$ , and it is several times higher than geometrical imperfections.

Zero detection with the automatic *AutoFind* method is evaluated as follows: tests are replicated ten times in different locations inside the  $10\text{ mm} \times 10\text{ mm}$  controlled area of the specimen. Table 3 summarizes experimental results given by the software, where  $z$  positions indicate the zero level settled on the specimen surface.

The standard deviation on these measurements is  $\sigma_{AF} = 43.7$   $\mu\text{m}$  and it is several times higher than the error connected to geometrical imperfections. This means that the variability in quote of zero reported in Table 3 are not (or not only) correlated with specimen surface irregularities. Delay between surface detection, cutter stopping and  $z$  quote measurement could explain this large error.

Table 3. Quote of zero point detected by *AutoFind* method.  
Tabela 3. Vrednosti nulte tačke detektovane metodom *AutoFind*

no.	1	2	3	4	5	6	7	8	9	10
Z ( $\mu\text{m}$ )	17.7	-45.5	32.2	-29.1	48.9	-46.8	23.6	-21.9	57.0	78.4

Finally, *Multimeter* method is adopted and ten measurements of zero point are executed. Results are reported in Table 4.

The standard deviation on these measurement is  $\sigma_T = 14.9$   $\mu\text{m}$ . That is to say that it is lower than the error associated to the previously illustrated methods and comparable with the error connected to the geometrical imperfections of the surface. It should be also considered that using this approach, no hole is produced while seeking the zero position, because the drilling system translates without rotating so that also the presence of a systematic error is avoided.

Table 4. Quote of zero point detected by *Multimeter* method.  
Tabela 4. Vrednosti nulte tačke detektovane metodom *Multimeter*

no.	1	2	3	4	5	6	7	8	9	10
Z ( $\mu\text{m}$ )	25.0	15.9	-14.0	-14.1	-4.3	-11.4	21.0	-4.5	-10.5	-3.0

### Analysis of the influence of geometrical parameters

Stresses are measured by means of ESPI + HDM on a specimen subjected to 3-point bending load. Geometrical parameters are measured as described previously. Then an error on geometrical parameters is simulated and results are recalculated and compared in order to detect the error on stress values  $\Delta\sigma_{xx}$ .

Firstly, the effect of an error on the  $\alpha_1$  angle is evaluated. Figure 6 shows the calculated stress  $\sigma_{xx}$  for the measured value of  $\alpha_1 = 42.5^\circ$  and for the error affected values of  $40.5^\circ$  and  $44.5^\circ$ . Table 5 summarizes numerical results and the effects in terms of percentage error on the calculated stress profile with respect to  $\alpha_1 = 40.5^\circ$ .

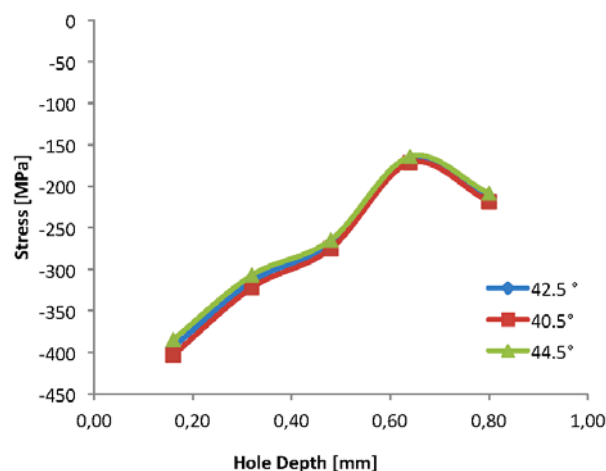


Figure 6. Calculated stress vs. the measured  $\alpha_1 = 40.5^\circ$  and hypothesizing an error of  $\Delta\alpha_1 = +2^\circ$  ( $42.5^\circ$ ) and  $\Delta\alpha_1 = -2^\circ$  ( $44.5^\circ$ ).

Slika 6. Sračunati napon i izmereno  $\alpha_1 = 40.5^\circ$  i hipotetička greška  $\Delta\alpha_1 = +2^\circ$  ( $42.5^\circ$ ) i  $\Delta\alpha_1 = -2^\circ$  ( $44.5^\circ$ )

Table 5. Calculated stress  $\sigma_{xx}$  for measured  $\alpha_1 = 40.5^\circ$  and  $\Delta\alpha_1 = \pm 2^\circ$ .

Percentage errors  $\Delta\sigma_{xx}$  are evaluated with respect to  $\alpha_1 = 40.5^\circ$ .

Tabela 5. Izračunati napon  $\sigma_{xx}$  za izmereno  $\alpha_1 = 40.5^\circ$  i za  $\Delta\alpha_1 = \pm 2^\circ$ .

Procentualne greške  $\Delta\sigma_{xx}$  su određene s obzirom na  $\alpha_1 = 40.5^\circ$

Hole depth (mm)	$\sigma_{xx}$ (MPa) $\alpha_1=42.5^\circ$	$\sigma_{xx}$ (MPa) $\alpha_1=40.5^\circ$	$\sigma_{xx}$ (MPa) $\alpha_1=44.5^\circ$	$\Delta\sigma_{xx}$ (%) $\Delta\alpha_1=-2^\circ$	$\Delta\sigma_{xx}$ (%) $\Delta\alpha_1=+2^\circ$
0.16	-393.5	-403.3	-384.5	2.49	2.29
0.32	-314.5	-322.0	-307.0	2.38	2.38
0.48	-268.3	-274.8	-264.3	2.42	1.49
0.64	-168.0	-171.8	-164.3	2.26	2.20
0.80	-213.5	-218.5	-208.5	2.34	2.34

The average error on the stress profile corresponding to an uncertainty of  $\Delta\alpha_1 = \pm 2^\circ$  is  $\overline{\Delta\sigma_{xx}}_{\alpha_1} = 2.26\%$ .

Secondly, the effect of an error on the  $\alpha_2$  angle is evaluated. Figure 7 shows the effect of an error  $\Delta\alpha_2 = \pm 2^\circ$  on the calculation of the stress profile  $\sigma_{xx}$  on a specimen under 3-point bending while in Table 6 are reported numerical results and the effects in terms of percentage error on the calculated stress profile.

The average error on the stress profile corresponding to an uncertainty of  $\Delta\alpha_2 = \pm 2^\circ$  is  $\overline{\Delta\sigma_{xx}}_{\alpha_2} = 4.98\%$ .

Thirdly, the effect of an error on the  $\beta_1$  angle is evaluated. Figure 8 shows the effect of an error  $\Delta\beta_1 = \pm 2^\circ$  on the

calculation of the stress profile  $\sigma_{xx}$  on a specimen under three-point bending while in Table 7 are reported numerical results and effects in terms of percentage error on the calculated stress profile.

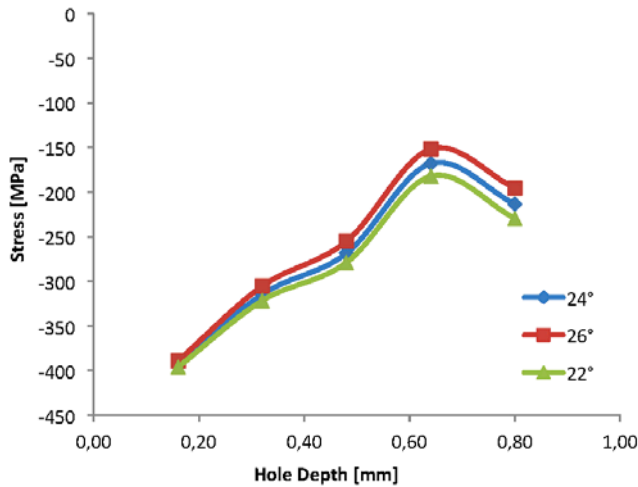


Figure 7. Calculated stress vs. measured  $\alpha_2$  (26°) and hypothesizing an error  $\Delta\alpha_2 = +2^\circ$  (24°) and  $\Delta\alpha_2 = -2^\circ$  (22°).

Slika 7. Izračunati napon i izmereno  $\alpha_2$  (26°) i hipotetičke greške  $\Delta\alpha_2 = +2^\circ$  (24°) i  $\Delta\alpha_2 = -2^\circ$  (22°)

Table 6. Calculated stress  $\sigma_{xx}$  for measured  $\alpha_2 = 24^\circ$  and  $\Delta\alpha_2 = \pm 2^\circ$ .

Percentage errors  $\Delta\sigma_{xx}$  are evaluated with respect to  $\alpha_2 = 24^\circ$

Tabela 6. Izračunati napon  $\sigma_{xx}$  za izmereno  $\alpha_2 = 24^\circ$  i za  $\Delta\alpha_2 = \pm 2^\circ$ .

Procentualne greške  $\Delta\sigma_{xx}$  su određene s obzirom na  $\alpha_2 = 24^\circ$

Depth (mm)	$\sigma_{xx}$ (MPa) $\alpha_2=24^\circ$	$\sigma_{xx}$ (MPa) $\alpha_2=22^\circ$	$\sigma_{xx}$ (MPa) $\alpha_2=26^\circ$	$\Delta\sigma_{xx}$ (%) $\Delta\alpha_2=-2^\circ$	$\Delta\sigma_{xx}$ (%) $\Delta\alpha_2=+2^\circ$
0.16	-393.5	-396.0	-388.8	0.63	1.19
0.32	-314.5	-321.5	-305.3	2.22	2.92
0.48	-268.3	-278.8	-255.0	3.91	4.96
0.64	-168.0	-182.0	-151.7	8.33	9.70
0.80	-213.5	-229.5	-195.5	7.49	8.43

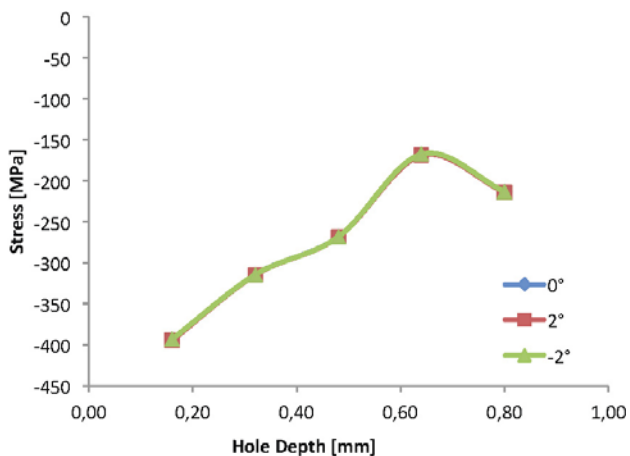


Figure 8. Calculated stress vs. measured  $\beta_1$  (2°) and hypothesizing an error  $\Delta\beta_1 = +2^\circ$  (0°) and  $\Delta\beta_1 = -2^\circ$  (-2°).

Slika 8. Izračunati napon i izmereno  $\beta_1$  (2°) i hipotetičke greške  $\Delta\beta_1 = +2^\circ$  (0°) i  $\Delta\beta_1 = -2^\circ$  (-2°)

The average error on the stress profile corresponding to an uncertainty of  $\Delta\beta_1 = \pm 2^\circ$  is  $\overline{\Delta\sigma_{xx}}_{\beta_1} = 0.17\%$ .

The effect of an error on the  $\beta_2$  angle is then evaluated. Figure 9 shows the effect of an error  $\Delta\beta_2 = \pm 2^\circ$  on the calculation of the stress profile  $\sigma_{xx}$  on a specimen under three-point bending while in Table 8 are numerical results and effects in terms of percentage error on the calculated stress profile.

Table 7. Calculated stress  $\sigma_{xx}$  for measured  $\beta_1 = 0^\circ$  and  $\Delta\beta_1 = \pm 2^\circ$ .

Percentage errors  $\Delta\sigma_{xx}$  are evaluated with respect to  $\beta_1 = 0^\circ$ .

Tabela 7. Izračunati napon  $\sigma_{xx}$  za izmereno  $\beta_1 = 0^\circ$  i za  $\Delta\beta_1 = \pm 2^\circ$ .

Procentualne greške  $\Delta\sigma_{xx}$  su određene s obzirom na  $\beta_1 = 0^\circ$

Depth (mm)	$\sigma_{xx}$ (MPa) $\beta_1=0^\circ$	$\sigma_{xx}$ (MPa) $\beta_1=-2^\circ$	$\sigma_{xx}$ (MPa) $\beta_1=+2^\circ$	$\Delta\sigma_{xx}$ (%) $\Delta\beta_1=-2^\circ$	$\Delta\sigma_{xx}$ (%) $\Delta\beta_1=+2^\circ$
0.16	-393.5	-394.3	-393.3	0.20	0.05
0.32	-314.5	-314.8	-314.5	0.10	0.00
0.48	-268.3	-268.5	-268.3	0.07	0.00
0.64	-168.0	-169.0	-167.5	0.60	2.20
0.80	-213.5	-213.8	-213.0	0.14	2.34

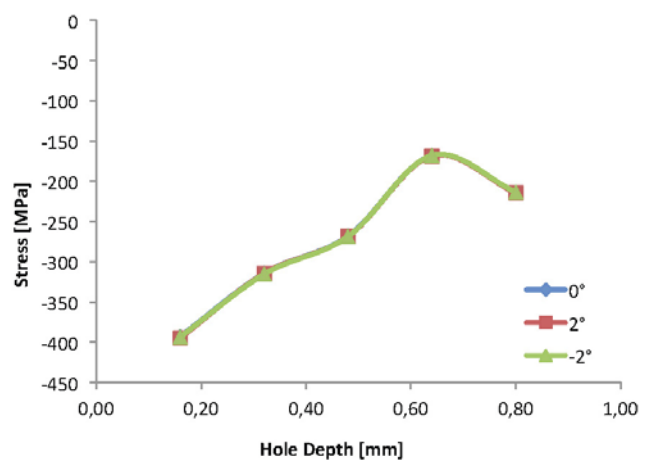


Figure 9. Calculated stress  $\sigma_{xx}$  for measured  $\beta_2$  (0°) and for  $\Delta\beta_2 = \pm 2^\circ$ . Percentage errors  $\Delta\sigma_{xx}$  are evaluated with respect to  $\beta_2 = 0^\circ$ .

Slika 9. Izračunati napon  $\sigma_{xx}$  za izmereno  $\beta_2$  (0°) i za  $\Delta\beta_2 = \pm 2^\circ$ .

Procentualne greške  $\Delta\sigma_{xx}$  su izračunate u odnosu na  $\beta_2 = 0^\circ$

Table 8. Calculated stress  $\sigma_{xx}$  for measured  $\beta_2 = 0^\circ$  and  $\Delta\beta_2 = \pm 2^\circ$ .

Percentage errors  $\Delta\sigma_{xx}$  are evaluated with respect to  $\beta_2 = 0^\circ$ .

Tabela 8. Izračunati napon  $\sigma_{xx}$  za izmereno  $\beta_2 = 0^\circ$  i za  $\Delta\beta_2 = \pm 2^\circ$ .

Procentualne greške  $\Delta\sigma_{xx}$  su određene s obzirom na  $\beta_2 = 0^\circ$

Depth (mm)	$\sigma_{xx}$ (MPa) $\beta_2=0^\circ$	$\sigma_{xx}$ (MPa) $\beta_2=-2^\circ$	$\sigma_{xx}$ (MPa) $\beta_2=+2^\circ$	$\Delta\sigma_{xx}$ (%) $\Delta\beta_2=-2^\circ$	$\Delta\sigma_{xx}$ (%) $\Delta\beta_2=+2^\circ$
0.16	-393.5	-393.8	-395.0	0.08	0.38
0.32	-314.5	-315.5	-314.8	0.32	0.10
0.48	-268.3	-268.8	-268.8	0.19	0.19
0.64	-168.0	-168.0	-168.5	0.0	0.30
0.80	-213.5	-213.5	-214.5	0.0	0.47

The average error on the stress profile corresponding to an uncertainty of  $\Delta\beta_2 = \pm 2^\circ$  is  $\overline{\Delta\sigma_{xx}}_{\beta_2} = 0.20\%$ .

Finally, the effect of an error on the  $\gamma_2$  angle is evaluated. Figure 10 shows the effect of an error  $\Delta\gamma_2 = \pm 2^\circ$  on the calculation of the stress profile  $\sigma_{xx}$  on a specimen under three-point bending while in Table 9 are the reported numerical results and the effects in terms of percentage error on the calculated stress profile.

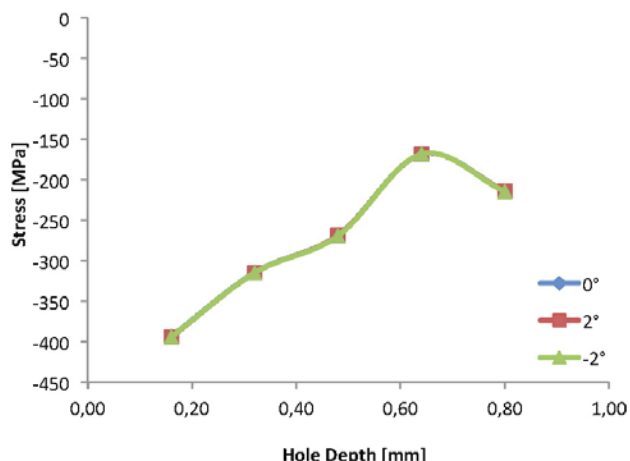


Figure 10. Calculated stress vs. measured  $\alpha_1$  ( $2^\circ$ ) and hypothesizing an error  $\Delta\gamma_2 = +2^\circ$  ( $0^\circ$ ) and  $\Delta\gamma_2 = -2^\circ$  ( $-2^\circ$ ).

Slika 10. Izračunati napon prema izmerenom  $\alpha_1$  ( $2^\circ$ ) i hipotetičke greške  $\Delta\gamma_2 = +2^\circ$  ( $0^\circ$ ) i  $\Delta\gamma_2 = -2^\circ$  ( $-2^\circ$ )

Table 9. Calculated stress  $\sigma_{xx}$  for measured  $\gamma_2 = 0^\circ$  and  $\Delta\gamma_2 = \pm 2^\circ$ .

Percentage errors  $\Delta\sigma_{xx}$  are evaluated with respect to  $\gamma_2 = 0^\circ$ .

Tabela 9. Izračunati napon  $\sigma_{xx}$  za izmereno  $\gamma_2 = 0^\circ$  i za  $\Delta\gamma_2 = \pm 2^\circ$ .

Procentualne greške  $\Delta\sigma_{xx}$  su određene s obzirom na  $\gamma_2 = 0^\circ$

Depth (mm)	$\sigma_{xx}$ (MPa)	$\sigma_{xx}$ (MPa)	$\sigma_{xx}$ (MPa)	$\Delta\sigma_{xx}$ (%)	$\Delta\sigma_{xx}$ (%)
	$\gamma_2=0^\circ$	$\gamma_2=-2^\circ$	$\gamma_2=+2^\circ$	$\Delta\gamma_2=-2^\circ$	$\Delta\gamma_2=+2^\circ$
0.16	-393.5	-394.0	-394.3	0.13	0.20
0.32	-314.5	-314.8	-314.8	0.10	0.10
0.48	-268.3	-269.0	-268.5	0.26	0.07
0.64	-168.0	-168.0	-168.3	0.0	0.18
0.80	-213.5	-214.3	-213.5	0.37	0.05

The average error on the stress profile corresponding to an uncertainty of  $\Delta\gamma_2 = \pm 2^\circ$  is  $\overline{\Delta\sigma_{xx}}_{\gamma_2} = 0.15\%$ .

## CONCLUSIONS

In this work the influence of errors on the knowledge of geometrical parameters is studied. In particular it is found that a  $\pm 2^\circ$  error in the knowledge of the in-plane  $\alpha_1$  illumination angle can introduce a 2% error on the measured stress while a  $\pm 2^\circ$  of the in-plane detection angle  $\alpha_2$  can introduce a 5% error on the measured stress profile. Less critical appears the knowledge of the out-of-plane angles. Three different zero detection procedures are also compared. The method based upon the use of a multimeter to detect electrical contact between driller and specimen is found to provide repeatability in the detection comparable with the geometrical irregularities of the analysed sample avoiding at the same time the introduction of a systematic error due to the drilling of a pre-hole while looking for the zero position.

## REFERENCES

1. Lasmis, J.L., *Prestress Engineering of Structural Material: A Global Design Approach to the Residual Stress Problem*, in Handbook of Residual Stress and Deformation of Steel, Eds. G. Totten, M. Howes, T. Inoue, Materials Park, OH, ASM International, 2002.
2. Schajer, G.S., Roy, G., Flaman, M.T., Lu, J., *Hole drilling and ring core methods*, in Handbook of Measurement of Residual Stresses, Ed. L. Jian, Bethel, Society for Experimental Mechanics, pp.5-35, 1996.
3. Schajer, G.S., *Advances in hole-drilling residual stress measurements*, Experimental Mechanics, 50(2):159-168, 2009.
4. Standard test method for determining residual stresses by the hole drilling strain-gage method, American Society for Testing and Materials, West Conshohocken, Standard E837-08, 2008.
5. Nelson, D.V., *Residual Stress Determination by Hole Drilling Combined with Optical Methods*, Experimental Mechanics, 50(2):145-158, Feb. 2010.